Scaling Behavior of Swollen Chains in Bimodal Molecular Weight Blends

Michael R. Landry

Imaging Research and Advanced Development, Eastman Kodak Company, Rochester, New York 14650-2132

Received February 27, 1997; Revised Manuscript Received August 15, 1997[⊗]

ABSTRACT: The phenomenon of swelling of several long polymer chains (length N), mixed at concentrations below c^* in a series of shorter chain "solvents" (length P), has been quantitatively studied by small-angle neutron scattering. The blends consist of perdeuterated polystyrene guest chains (M_w = 87 000−2 950 000), in hydrogenous PS hosts (M_w = 2 530−2 000 000). Scaling relationships have been established for the long chain's radius of gyration R_g and second virial coefficient A_2. For bimodal blends where the long chain is in the unswollen regime ($P > N^{1/2}$), the scaling is that of a random walk chain, with $R_g \sim N^{0.504\pm0.009}$ and $A_2 \sim P^{-0.95\pm0.24}$. For the swollen regime, one observes $R_g \sim N^{0.59\pm0.02}P^{-0.10\pm0.02}$ and $A_2 \sim N^{-1/5}P^{-0.59\pm0.10}$. The weaker than predicted dependence of R_g on P, $-1/10$ vs $-1/5$ from theory, implies that in the swollen regime, the screening blob size ξ depends on $P^{1/2}$ rather than P as originally hypothesized. The approximate crossover point at qR_g(short) ≈ 1 in the static structure factor of the long chain from $S(q) \sim q^{-1.7}$ for large distances (excluded volume) to ideal chain statistics $S(q) \sim q^{-2}$ at smaller scales is seen as a confirmation of the screening effect of the short chains.

I. Introduction

Common to all linear high polymers is their threadlike nature. The topological interaction of polymer chains in the melt state or in solution is unique in the area of materials science. Each chain's local environment is occupied by not only its own segments but also parts of other chains and/or solvent molecules. The entropic and enthalpic interactions between a macromolecule and its surroundings often dictate its final conformation. An example is in dilute solutions, where depending on the relative segment−segment and segment−solvent interactions, a polymer chain's conformation may be completely collapsed (globular), "ideal" (unperturbed random walk), swollen (self-excluding random walk), or even rodlike (for a charged polyelectrolye with no added salt). The other concentration extreme is in the melt state, where each chain adopts the ideal conformation, that is, a Brownian random walk trajectory of statistical segments along its contour length, which essentially results in a Gaussian segment density distribution about the center-of-mass.[1] The static properties of polymers in solution has received vast attention on both theoretical and experimental fronts.[2] The following is a digest that is germane to this study.

We have chosen to examine "conventional" macromolecules, *i.e.*, linear, nonpolyelectrolytes. According to simple scaling descriptions for an ideal polymer chain undergoing an unperturbed random walk, the monomer pair correlation function $g(r)$ and its Fourier transform $S(q)$ scale as[3]

$$g(r) \sim r^{-1} \tag{1}$$

$$S(q) \sim q^{-2} \tag{2}$$

for the approximate interval $R_g > r > b$, with R_g and b representing the radius of gyration and the statistical segment length, respectively. The magnitude of scattering vector, q, is a length scale in reciprocal space whose magnitude is defined by the type of radiation in a light-, X-ray-, or neutron-scattering experiment. Ultimately, the overall chain size as measured by R_g varies with the number of chain segments N according to

$$R_g \sim N^{1/2} \tag{3}$$

The scaling relationship represented by eq 3 was confirmed several decades ago for dilute solutions at the Flory Θ-temperature via intrinsic viscosity measurements.[4] It has been also observed by direct measurements of R_g by light scattering.[5,6] At the other concentration extreme, polymer chain dimensions in melts of chemically identical, monodisperse chains[7,8] studied by small-angle neutron scattering (SANS) have been seen to agree with eq 3. With respect to chain conformation at intermediate length scales, the q-dependence given in eq 2 has been seen in melts[7,9] and at the Θ-point.[5,7,10] For the dilute solution case, it is a balance of the attractive and repulsive two-body interactions between polymer and solvent monomers that leads to the unperturbed random walk of the statistical segments, characterized by Brownian statistics of the backbone trajectory. For the melt, the pervading monomers of neighboring chains screen the repulsions of monomers of any given chain. The diminution of interactions is characterized by a vanishing second virial coefficient A_2.[2−4]

When there is a net increase of repulsive interactions along the chain it swells until there is a balance with the energy of elastic deformation.[1] One can arrive at this point by either increasing the temperature from the Θ-point (in dilute solutions) or by adding a monomeric solvent to the melt until the dilute solution limit is reached (concentration $c <$ overlap concentration c^*, for $T > \Theta$). The result for the good solvent limit as $N \rightarrow \infty$ is a swollen coil with the scaling relationships[3,11,12]

$$g(r) \sim r^{-4/3} \tag{4}$$

$$S(q) \sim q^{-5/3} \tag{5}$$

[⊗] Abstract published in *Advance ACS Abstracts,* November 1, 1997.

S0024-9297(97)00270-2 CCC: $14.00

$$R_g \sim N^{3/5} \quad (6)$$

The results of early small-angle neutron scattering experiments are consistent with the excluded volume exponent shown in eq 5 for the intermediate q-range,[7,13] although the local structure of the polymer chains as one approaches $q \sim 1/b$ must carefully be considered.[14] Excluded volume exponents determined from the molecular weight dependence of R_g in eq 6 have also been recorded.[5,6,15]

Apart from the asymptotic scaling behavior for unperturbed and excluded volume chains, there also exist crossovers for intermediate conditions. The transition to a swollen coil is not uniform over all length scales. In going from the melt toward dilute solution, R_g of each chain gradually increases. A concentration-dependent crossover in the correlation of monomers is seen via a structure factor change from $S(q) \sim q^{-5/3}$ toward $S(q) \sim q^{-2}$ as one proceeds from high to low q, indicating that the chain statistics are "ideal" at long length scales, and self-avoiding at shorter ones.[16] Likewise, a crossover is predicted as the temperature is raised from the Θ-point; however, the trend in monomer distribution is reversed, with $S(q)$ changing from q^{-2} to $q^{-5/3}$ when going from short to long spatial scales, that is, from high to low q. Both concentration and temperature-dependent crossover results have been seen in small-angle neutron scattering experiments.[17]

What happens to the single polymer chain composed of N segments when the solvent *molecular weight* (P segments) is decreased to that of a monomer from the melt state? This problem was originally examined by Flory in 1949[1] and more recently revisited by de Gennes.[18] Scaling predictions have been proposed for more general situations, such as the incorporation of a small molecule solvent,[19] polydispersity,[20] and the possibility of (in)compatability between chains N and P.[21] For this paper we focus on the simplest case of bimodal "molecular weight blends" in the melt state, where dilute long chains (guest, solute, length N) are at concentrations c_N less than the overlap concentration c_N^* and are dissolved in chemically identical short ones (host, solvent, length P).

It has been predicted that the guest chain's R_g will undergo a crossover from an unswollen to a swollen state in the vicinity[1,18]

$$P \approx N^{1/2} \quad (7)$$

as one decreases the "solvent" length P. This crossover point was deduced from examination of the Flory free energy of the long chain as having an elastic contribution due to its expansion (stretching), and an excluded volume interaction term controlled by the short chains. Excluded volume interactions between the guest chain segments become prevalent, with the second virial coefficient A_2 increasing simultaneously. The long chain R_g and A_2 are predicted to follow the scaling relationships[19−21]

$$R_g \sim N^{3/5}P^{-1/5}, \quad A_2 \sim N^{-1/5}P^{-3/5} \; (P < N^{1/2}) \quad (8)$$

$$R_g \sim N^{1/2}, \quad A_2 \sim P^{-1} \; (P > N^{1/2}) \quad (9)$$

Accompanying these global scaling changes should be a transition from Brownian to excluded volume statistics for the segment−segment correlations of the guest chains. On the small distance side of the crossover point defined in eq 7, the monomer distribution of the guest chain should be ideal, with $S(q) \sim q^{-2}$. At longer distances, one should observe a $q^{-5/3}$ dependence.[19b−21] The length scale for this crossover is thought to depend *linearly* on the number of segments P in the short chain, that is, its contour length, rather than on $P^{1/2}$ which would be the case for a dependence on the short chain's radius of gyration. The precise position of the crossover has been the subject of a recent theoretical investigation.[22]

Evidence of swelling of a long chain in a binary "molecular weight" blend has been observed in SANS experiments by Kirste and Lehnen[23] for poly(dimethylsiloxane) and Tangari *et al.*[24] for polystyrene, albeit for a *single* guest chain of length N. In both of these studies, the concentration of the long chains were sufficiently dilute such that only long chain/short chain interactions dominated. Other studies of bimodal molecular weight blends have been reported;[25,26] however, the concentrations of the long chains were sufficiently high (ca. 10−40 vol %) such that segment−segment interference between separate long chains was significant, thereby preventing any of the measured chain dimensions to be considered in this study. Swelling due to a short host polymer has also been observed in a unique ternary system of polystyrene (guest)/poly(methyl methacrylate) (host)/good solvent over and above the effect due to the small molecule solvent by light scattering.[27] Each of these groups clearly demonstrate an increase of R_g and A_2 upon a decrease of matrix size P. In fact, several recent theories of chain conformation at interfaces between high and low molecular weight polymers,[28] chain transport through gels,[29] and dynamics in bimodal blends[30] assume that chain swelling occurs and that the Flory condition for swelling of a long chain addressed in eq 7 holds. Similarly, the phenomenon has been used to explain some experimental polymer interdiffusion results.[31,32] This study affords an opportunity to test certain assumptions regarding the scaling of swollen chains in bimodal melts that have been, up to this point, accepted with minimal experimental confirmation.

II. Experimental Section

SANS Experiments. Materials and Sample Preparation. Six samples of polystyrene-d_8 (dPS) of varying molecular weight and narrow polydispersity were obtained from Polymer Laboratories Inc., Amherst, MA. These were combined with several lower molecular weight hydrogenous samples (hPS) purchased from Pressure Chemical Co., Pittsburgh, PA. The characterization data for the samples and a summary of the blend pairs are given in Table 1. With the exception of the highest molecular weight dPS and hPS samples (2 950 000 and 2 000 000, respectively), all molecular weight characterization was performed in-house by size-exclusion chromatography (SEC) in tetrahydrofuran (THF) using three 10-μm mixed-bed columns.

For the blends used to obtain R_g and A_2, each consisted of three dPS concentrations, which are shown in Table 1. The blend designations indicate the deuterium-labeled polymer D weight-averaged molecular weight followed by the unlabeled hydrogenous H molecular weight. The final blend preparation entailed dissolving the premeasured mixed powders into either toluene or tetrahydrofuran to ca. 2−10% by weight depending on the host molecular weight. The solutions were passed through 0.45 mm filters prior to precipitation into a large excess of methanol (for the THF solutions) or a 50/50 mixture of methanol/2-propanol (toluene solutions). The precipitates were collected and dried under vacuum at 60−80 °C until constant weight.

Table 1. Molecular Weight Characterization and Blend Pair Summary

Fig 4&8	hPS (host)			*P/N* pairs					
Symbols	10^3M_w	M_w/M_n	[a]*P*	D2950	D514	D251	D183	D107	D87.8
	H2000	< 1.20	3846	x					
	H180	1.03	346		x				
	H115	1.03	221	x	x	x	x		
	H51.3	1.04	98.6		x				
	H39.4	1.04	75.8	x	x		x		
	H22.1	1.05	42.5	x	x	x		x	
	H11.2	1.09	21.5	x	x	x			
	H3.69	1.10	7.10	x	x	x	x	x	
	H2.53	1.26	4.86			x	x		x

Fig 9&10	dPS (guest)			blend concentrations	hPS crossover
Symbols	10^3M_w	M_w/M_n	[b]*N*	(wt % dPS)	10^3M
	D2950	1.11	5270	0.5	37.7
	D514	1.11	918	0.5, 1.0, 2.0	15.7
	D251	1.11	448	1.0, 2.0, 3.0	11.0
	D183	1.04	327	1.0, 2.0, 3.0	9.4
	D107	1.04	191	1.0, 2.0, 3.0	7.2
	D87.8	1.03	157	1.5, 3.0, 4.5	6.5

[a] Calculated from Kuhn segment molecular weight $M_K = 520$. [b] Calculated from Kuhn segment molecular weight $M_K = 560$.

The final blend specimens for the scattering experiments were prepared in two ways. For samples with the three lowest molecular weight hPS matrices, the dried powders were compacted into 1 cm diameter tablets for ease of handling, placed inside a $^5/_8$-inch i.d., $1^1/_4$ inch o.d., 1.6 mm thick Teflon washer, followed by melt pressing into transparent disks at a temperature of about 90−110 °C for $^1/_2$ to 1 h. Use of the Teflon washers lent support and lessened the development of cracks in these brittle samples. All of the remaining higher molecular weight blends were melt pressed into free-standing disks, $^1/_2$ to $^3/_4$ in. diameter and 1 to 1.25 mm thick, employing molds connected to a house vacuum. Molding temperatures for these samples tended to be between 120−130 °C. The mold assembly used for melt pressing had a sidearm that was connected to a house vacuum line which served to minimize bubble formation in the samples.

Scattering Geometries and Measurements. The blend samples and hPS and dPS blanks were examined by SANS under ambient conditions at the research reactor of the National Institute of Standards and Technology (NIST). Because this study commenced in 1986 and has been recently completed, measurements have been carried out on several of the NIST small-angle spectrometers. Early experiments in 1986 were performed on the blends containing dPS M_w = 251 000 employing the 8 m instrument with focusing collimation[33] and a neutron wavelength $\lambda = 5.90$ Å, $\Delta\lambda = 1.5$ Å. At the time, this configuration afforded the best balance between incident beam flux (the cold source had not yet been installed) and the smallest possible scattering vector $q = 0.0069$ Å^{-1}, with $q = (4\pi/\lambda)\sin(\theta/2)$. Acquisition times were from 2 to 6 h per sample because of the low labeled polymer content.

Subsequent experiments (1992 and 1993) were carried out on either the 30 m NIST/Exxon/UMinn NG7-SANS or the NIST/NSF NG3-SANS spectrometers. Nominal sample-to-detector distances SDD were 15, 8, and 3 m. The neutron wavelength was set at $\lambda = 6.00$ Å, $\Delta\lambda/\lambda = 0.34$. Data acquisition times were reduced to $^1/_2$ h up to ca. 3 h, depending on the SDD and the amount of labeled polymer. The largest SDD provided a minimum q of 0.0036 Å^{-1} necessary to evaluate the R_g for the D514 blends. To access the broadest q-range as possible to investigate the crossover effect in the single chain structure factor, both the shortest (3.56 m) and the longest (13.0 m, NG3; 15.3 m, NG7) SDD allowed for the broadest range of $q = 0.0036-0.125$ Å^{-1}.

Preliminary Data Treatment. All data were treated according to standard procedures for isotropic scattering. The measured intensities were corrected for area detector nonuniformity using the scattering from H_2O and beam-blocked background using ^{6}Li glass (30 m camera on NG3 and NG7) or Cd sheet (8 m camera). The incoherent scattering due to the large amount of protons within the blend samples was subtracted using the scattering from various hPS blanks, appropriately weighted by the relative sample thicknesses, transmission, and percent hPS. Since the deuterium content was low, the incoherent scattering from dPS was usually neglected. After the data were azimuthally averaged by employing suitable masks to ignore channels from the detector perimeter and beamstop location, they were placed on an absolute intensity scale as the differential scattering cross section $d\Sigma(q)/d\Omega$ (units cm^{-1}) by rescaling with secondary standard samples (a silica gel standard for the 8 m instrument,[34] and the SDD = 8 m runs on NG7; H_2O in a 1 mm quartz cell for SDD = 3.56 m runs on both NG7 and NG3; a 50/50 blend of hPS/dPS for the SDD = 13 m and 15.3 m runs on NG3 and NG7, respectively). The analysis procedures used to extract molecular weight, radius of gyration, and the second virial coefficient are discussed in the Results.

III. Results

A. Analysis of SANS Data. With one of the goals of this study being to test the scaling relationships of R_g and A_2 as functions of the guest and host molecular weights, it is essential to obtain accurate values for these parameters. There are several separate issues that require discussion before examination of the final results. First, the details of the analysis methods used to extract R_g, A_2, and M_w are described and scrutinized. The possibility of systematic influences on these quantities is addressed. Second, the question of blend incompatibility due to isotopic substitution and possible chain end effects is discussed with the input of known experimental results. Finally, a short evaluation of the effect of the host polymer glass temperature is given.

Chain Structure Factor Analysis. With respect to the analysis methods, a combination of two approaches is used for SANS data evaluation. Each method weights the scattering profiles differently, giving slightly different results. So as not to bias any of the final values, the results are averaged to produce the final numbers. A numerical summary of the analyses is given in Table 2.

The first approach is based on the Zimm plot method.[35] In the usual Zimm plot, one plots for each concentration of perdeuterated polymer the quantity $Kc/[d\Sigma(q)/d\Omega]$ vs $q^2 + kc$, where k is an arbitrary constant and K contains the sample contrast factors. With the intensity data converted to an absolute scale, $K = N_o\rho[(a_{dPS} - a_{hPS})/M_{dPS}]^2$. N_o is Avogadro's number, ρ is the density (=1.05 g cm^{-3}, assuming no change upon mixing), a_{dPS} and a_{hPS} are the monomer scattering lengths (=10.7×10^{-12} and 2.32×10^{-12} cm, respectively), and M_{dPS} is the monomer molecular weight. After the appropriate extrapolations are performed, R_g is retrieved from the slope and intercept of the $c = 0$ line ($R_g = (3 \times \text{slope/intercept})^{1/2}$), A_2 from the slope of the $q = 0$ line (slope $= 2A_2\rho$), and M_w from the double extrapolation to the abscissa intercept ($M_w = 1$/intercept). If the data cover enough of a range below $qR_g = 1$ for the $c = 0$ plot, then the analysis is independent of chain conformation. This approach was used by Kirste and Lehnen[23] in the original SANS experiment where chain swelling in bimodal blends was first noted.

For the samples in this study, the $qR_g = 1$ limit is often exceeded, particularly when chain swelling occurs. To remedy this, a modified approach as espoused by Ullman[36,37] is employed. First, Zimm plots for the three

Table 2. Measured Values of R_g, A_2, and M

	R_g (Å)				A_2 (10^{-5} cm^3 mol/g^2)			M_w (10^3 g/mol)		
blend pair	Zimm	Debye	Debye (c=0)	av	Zimm	Debye	av	Zimm	Debye	av
D514H180	187 ± 12	183 ± 6	188 ± 5	186	−0.34 ± 0.25	−0.36 ± 1.08	−0.35	562 ± 32	463 ± 32	512
D514H115	178 ± 12	185 ± 3	196 ± 8	186	0.31 ± 1.27	0.80 ± 1.37	0.55	520 ± 29	462 ± 46	491
D514H51.3	172 ± 17	188 ± 11	189 ± 8	185	1.05 ± 1.23	1.88 ± 1.06	1.47	699 ± 56	589 ± 57	644
D514H39.4	187 ± 9	182 ± 1	188 ± 4	186	1.39 ± 0.06	1.41 ± 0.06	1.40	554 ± 19	509 ± 44	532
D514H22.1	190 ± 9	185 ± 6	192 ± 6	189	1.95 ± 0.04	1.93 ± 0.24	1.94	554 ± 20	503 ± 16	528
D514H11.2	212 ± 23	195 ± 15	211 ± 9	206	5.25 ± 0.69	5.21 ± 0.95	5.23	682 ± 66	560 ± 48	621
D514H3.69	217 ± 40	201 ± 33	220 ± 10	213	8.97 ± 2.37	9.81 ± 2.49	9.39	638 ± 96	565 ± 50	601
D251H115	129 ± 7	128 ± 9	127 ± 1	128	0.63 ± 0.35	0.63 ± 1.1	0.63	301 ± 15	210 ± 10	256
D251H22.1	134 ± 20	129 ± 3	129 ± 3	131	3.48 ± 1.43	3.11 ± 1.81	3.30	369 ± 50	212 ± 20	291
D251H22.1	132 ± 16	131 ± 4	132 ± 2	132	3.37 ± 0.76	3.51 ± 0.95	3.44	392 ± 33	197 ± 7	244
D251H11.2	133 ± 9	135 ± 1	137 ± 3	135	4.09 ± 0.33	4.87 ± 0.32	4.48	272 ± 17	193 ± 4	232
D251H3.69	153 ± 18	139 ± 2	149 ± 2	147	12.5 ± 0.7	12.0 ± 0.8	12.25	328 ± 34	187 ± 8	257
D251H2.53	171 ± 9	150 ± 4	177 ± 5	166	9.89 ± 1.46	9.19 ± 1.84	9.54	257 ± 94	212 ± 15	234
D183H115	102 ± 2	109 ± 3	108 ± 1	107	−0.57 ± 0.45	−0.42 ± 0.09	−0.49	186 ± 2	176 ± 2	182
D183H39.4	107 ± 4	113 ± 1	111 ± 1	110	0.25 ± 0.44	0.46 ± 0.32	0.35	189 ± 6	173 ± 3	181
D183H3.69	114 ± 8	120 ± 1	117 ± 2	117	7.46 ± 0.04	8.90 ± 0.18	8.18	200 ± 9	196 ± 3	198
D183H2.53	125 ± 8	120 ± 14	131 ± 3	126	6.95 ± 0.03	8.51 ± 1.45	7.73	182 ± 9	172 ± 9	177
D107H22.1	94.9 ± 8.4	79.6 ± 3.2	81.4 ± 4.2	85.3	1.61 ± 1.87	1.57 ± 1.32	1.59	106 ± 5	100 ± 4	103
D107H3.69	93.1 ± 7.3	92.5 ± 4.4	95.9 ± 3.0	93.8	12.8 ± 3.09	11.6 ± 0.3	12.2	116 ± 2	105 ± 1	110
D87.8H2.53	78.6 ± 3.5	78.1 ± 7.5	81.1 ± 0.9	79.1	16.9 ± 2.2	16.9 ± 3.6	16.9	102 ± 5	73.2 ± 8	87.5

concentrations of each blend pair are constructed. The extracted R_g's are used to calculate the single-chain structure factor over the limited q range used for the Zimm plot, using a form of the Debye equation that has been modified with a Schultz−Flory−Zimm distribution[36] for the slight polydispersity

$$S(q) = \frac{2}{x}\left\{1 - \frac{z+1}{zx}\left[1 - \left(1 + \frac{x}{z+1}\right)^{-z}\right]\right\} \qquad (10)$$

Here, $x = (qR_g)^2$, and $M_w/M_n = (z+1)/z$. For reference, the Debye equation is provided[38]

$$S(q) = 2(e^{-x} + x - 1)/x^2 \qquad (11)$$

Using the recalculated structure factor, a value of R_g is then determined according to the Zimm approximation, that is, from $1/S(q)$ vs q^2. Because the radius values from the original Zimm plot and from the recalculated structure factor are not equal owing to qR_g not being at the asymptotic limit of $qR_g < 1$, its value is adjusted. The new R_g value is inserted into eq 10 to find a new $S(q)$ and the procedure iterated until the two radii of gyration are identical. The value of the Zimm plot intercept must also be recalculated in the same manner, as it is related to the guest polymer molecular weight. The effect of this procedure on the second virial coefficient A_2 is minor relative to the experimental uncertainty. Values for R_g, M_w, and A_2 using this approach are recorded in Table 2 in the column titled "Zimm". Figure 1 shows a Zimm plot for the blend D514H22.1, with every other data point being shown.

The second procedure is to fit the entire scattering profiles at each concentration to the Debye equation with polydispersity, using the formula

$$c^{-1}[d\Sigma(q)/d\Omega] = \alpha S(q) + \beta \qquad (12)$$

The fitting parameter β accounts for any incoherent background that may not have been accounted for in the preliminary data treatment. Typical values for β were <1% of α. The front factor α and R_g, depend on concentration, while no apparent correlation existed for β. The intercept of $1/\alpha$ vs c provides M_w; the slope gives A_2. Likewise, the radius of gyration must be extrapolated to $c = 0$. The final parameter determinations are listed in Table 2 under the heading "Debye". The cited uncertainties are from the result of the extrapolation step, which covers only three data points. Figure 2 displays fits to the SANS data for three concentrations of the blend D514H22.1. Note that the intensities (*i.e.*, $d\Sigma(q)/d\Omega$) have not been scaled for the guest polymer concentration in order to keep the curves separated.

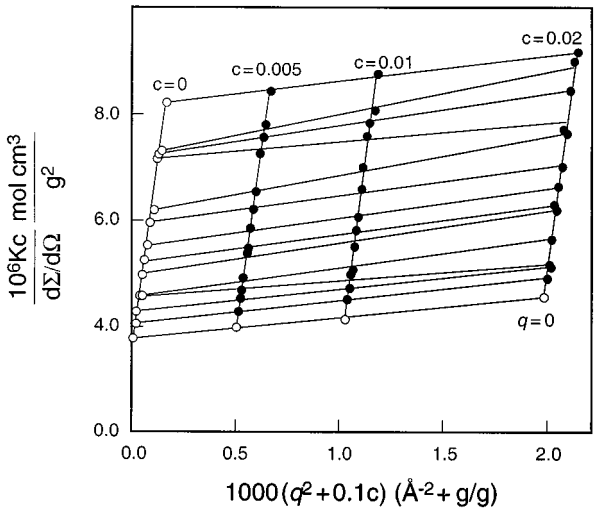

Figure 1. Zimm plot for the blend D514H22.1, with every other data point being shown.

The third analysis involves a combination of the Zimm and Debye methods. The reciprocal differential scattering cross sections (normalized for concentration) are extrapolated at each angle point-by-point to zero concentration to give a full scattering profile. The $c = 0$ data are then fit with the modified Debye equation (eq 10) with no added baseline term. See Figure 3 for a typical fit; note that the intensity scale is much greater than that in Figure 2 due to the normalization for concentration. Using this method, only values for R_g and M_w are obtained. Only the values for R_g are reported under the heading "Debye (c = 0)", as the results for M_w often coincide with those in the "Debye" column of Table 2.

Because R_g and M_w are very sensitive to the intensities recorded at the lowest q, some caution is required

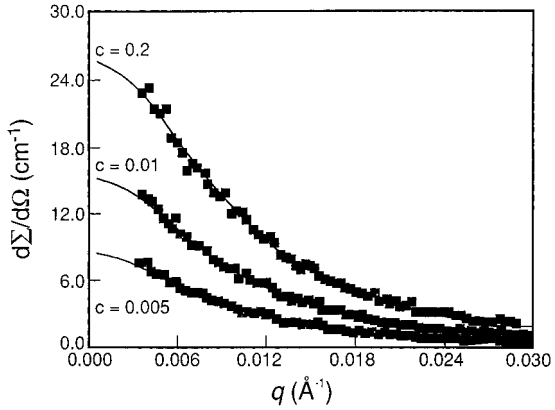

Figure 2. Fits to the SANS data for three concentrations of the blend D514H22.1 using eqs 10 and 12. Note that the intensities (*i.e.*, $d\Sigma(q)/d\Omega$) have not been scaled for the guest polymer concentration in order to keep the curves separated.

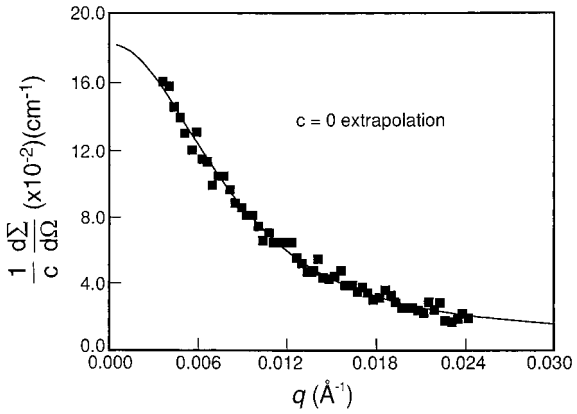

Figure 3. Fit of infinite dilution-extrapolated data for the blend D514H22.1 according to the modified Debye equation (eq 10) with no baseline term.

in fitting data. In this region there is increased uncertainty in the intensities because fewer detector channels are used for radial averaging, incident beam masking is crucial, and low signal-to-noise ratios are present due to very small amounts of labeled chain (down to 0.5 wt %). This is particularly relevant as chain swelling occurs, at which time the intensities become steeper at the low q end of a scattering profile. On occasion, some of the samples appear to show excess scattering at very low q, which has to be considered. Therefore, data points at the smallest angles were dropped successively for each of the analysis methods until very little change in the parameters was noted, and the fit quality did not suffer. For a majority of the data sets, very few, if any, points were neglected in the fits. However, for one sample, D251H51.3 (not shown in either Tables 1 or 2), no satisfactory fits were obtained in this fashion, thereby requiring the data to be discarded. These details, having been suggested previously,[39] are important when trying to eliminate prejudice from the study.

Another important factor to address is the use of the Debye function, derived for unperturbed chains having a Gaussian segment density distribution,[38] to describe the single chain structure factor, even for swollen chains. A systematically increasing difference between $R_{g,actual}$ and $R_{g,fit}$ may be introduced as the chain swells because the same formula for the single chain structure factor is used. From previous light-scattering[5] and neutron-scattering[40,41] experiments of polystyrene in good solvents, there is experimental justification for use of the Debye equation, and at this time there are no tractable analytical expressions for the structure factor of excluded volume chains. Moreover, as reported by Tangari *et al.*,[24] precedence on theoretical grounds has also been extended.[42,43] An effective check of sample preparation and data analysis is the comparison of the dPS M_w from the SANS experiments (last column of Table 2) to the independently determined SEC values (first column, numerical suffix to the letter D in the blend designations). The molecular weights determined from Zimm plots are always greater than those from the Debye equation fits, yet there is no systematic change of SANS M_w as the host polymer is varied. In fact the two quantities tend to bracket the SEC value, resulting in agreement between the first and last columns. Some discrepancy is noted for the dPS molecular weight in the D514 blend series in that most of the quantities measured by SANS exceed the SEC value. However, it is again mentioned that there is no systematic trend with respect to host molecular weight using either method. The difference between the Zimm and Debye fits is attributed to the way the data are weighted by the fit procedures, and is another reason why each approach is cited. Interestingly, there are no similar disparities in either R_g or A_2. It is therefore concluded that the analysis methods are reasonable for this study.

To close this portion of the structure factor analysis discussion, a few comments are in order as to why the random phase approximation (RPA)[3] was not used. For a miscible binary blend of chemically identical species having the same segmental molar volumes, the total scattering structure factor contains the reciprocal sum of the individual structure factors $S(q)$

$$\frac{K}{d\Sigma(q)/d\Omega} = \frac{1}{N\phi_d S_d(q)} + \frac{1}{P\phi_h S_h(q)} - 2\chi \qquad (13)$$

where N and P in this formalism are the degrees of polymerization, $\phi_{d,h}$ are the respective d and h volume fractions, and the Flory χ-parameter accounts for polymer−polymer interactions. Briber *et al.*[44] have indicated that the RPA expression is reduced to the classical Zimm form at dilute concentrations of the labeled component, with χ being incorporated into the second virial coefficient. This means that only the labeled component's radius of gyration is measured independently. Moreover for dPS/hPS blends, χ is too small to be distinguishable from zero within the experimental uncertainty of our data, therefore its affect on A_2 is also negligible. Thus one is led to the conclusion that the RPA would not provide additional information to the analysis.

Isotopic Compatibility. It has been suggested[45] that there is a small but finite repulsive interaction between deuterated and protonated polymers. A positive Flory χ-parameter has been measured for high molecular weight dPS/hPS mixtures by Bates and Wignall[46] with the temperature dependence[47]

$$\chi = 0.20/T - 2.9 \times 10^{-4} \qquad (14)$$

A phase diagram with a UCST is predicted for isotopic mixtures of polystyrene. To explore the consequences of the interaction parameter in eq 14, a simple calculation is done for the D514H180 blend to determine at what temperature instability is expected. For this exercise, the conventional free energy of mixing expression for a binary blend according to the Flory ap-

proximation,[3,4] is used. The volume fraction of the deuterated polymer ϕ_c and $(\chi N)_c$ at the critical point are

$$\phi_c = P^{1/2}/(N^{1/2} + P^{1/2}) \quad (15)$$

$$(\chi N)_c = (N^{1/2} + P^{1/2})^2/2P \quad (16)$$

Incorporating the degrees of polymerization (dp) for the long and short chain polymers of this blend, $\phi_c = 0.38$ and $(\chi N)_c = 3.46$. For the deuterated polymer D514 (dp = 4590), $\chi_c = 7.54 \times 10^{-4}$, yielding a critical point temperature of about −80 °C according to eq 14, well below the glass temperature for polystyrene. Since the blend compositions are far from the critical composition ϕ_c, isotopic incompatibility is not an issue. For all of the molecular weight pairs represented in Table 2 for which quantitative analysis for R_g and M_w is performed, the samples are well into the single phase region of the phase diagram.

The case is not as clear for the highest molecular weight combination, D2950H2000. Although the critical composition is shifted to $\phi_c = 0.46$, well away from the 0.5 wt % composition examined, $(\chi N)_c = 2.36$, which gives a UCST phase separation temperature T_c of approximately 250 °C at ϕ_c, calculated from the degree of polymerization. Thus it appears from these "back-of-the-envelope" calculations that homogeneous blends of the D2950H2000 pair can never be made if compositions near ϕ_c are desired. However, the coexistence curve in T vs ϕ space is concave downward for UCST systems; therefore, as one approaches $\phi = 0$ or 1, compatibility should be the rule. This is the only blend where instability may be of importance; for example, $T_c = -60$ °C at $\phi_c = 0.17$ for D2950H118. Since none of the samples with the high molecular weight D2950 are examined for R_g, the issue of blend compatibility is of secondary concern.

Chain End Effects. In a SANS study reported by O'Connor *et al.*[25] of bimodal blends of high and low molecular weight polystyrene, where the compositions of the high molecular weight component were between 10 and 50 vol %, deviations from ideal mixing behavior were observed. They postulated that the nonideal mixing arose from the significant contributions of the *n*-butyl terminated short chains (from the anionic polymerization) to the total mixing free energy. The worst case cited was for the pair D110/H1.05 (in the terminology of this study), where the SANS-measured χ was comparable in magnitude to the spinodal χ_s calculated according to the simple lattice model. Interestingly, the effect of the chain ends was to *decrease* the long chain's overall dimensions, which is opposite to the phenomenon addressed in this report. Nevertheless, it is noted that an extrapolation to where the chain end effect is negligible is 3300 g/mol for the short chain. In fact, values for the average statistical segment length in blends with 2150 or 2950 g/mol chains are comparable to values recorded in the literature for ideal chains.[25] It is concluded from these observations that there are no pertinent interfering effects on the long chain dimensions due to unfavorable enthalpic interactions caused by *n*-butyl terminated short chains.

Host Polymer T_g and Specific Volume. All of the samples were measured at ambient temperatures in the SANS spectrometers, which is below the glass transition temperatures of all of the samples. It is known that T_g has a significant dependence on molecular weight, which becomes especially evident for low molecular weights. Assuming that the dilute guest dPS does not contribute to the bulk thermal properties of the hPS host, the glass temperature for these blends drops from an asymptotic value of 93.5 to 53 °C for the lowest molecular weight extreme.[48] Therefore, a systematic change of labeled chain dimensions upon cooling from the preparation temperature to T_g, should be considered, assuming little change occurs once T_g is reached. However, the concomitant specific volume change with molecular weight is not as striking. According to empirical relationships between the glassy specific volume ν_g as a function of temperature and molecular weight deduced from volumetric measurements by Richardson and Savill,[48] $\nu_g(T_g) = 0.9695$ cm^3/g for H180 ($T_g = 93$ °C), 0.9688 cm^3/g for H22.1, and 0.9626 cm^3/g for H2.53 ($T_g = 53$ °C). This represents less than a 1% decrease of the glass volume; therefore, any shrinkage of R_g would certainly be undetectable from the SANS measurements. It has already been shown in the earliest SANS studies on polystyrene,[9] where measurement uncertainty is reported to be within 5%, that there is an imperceptible change of R_g with temperature over the range 20−160 °C. More recent precise measurements on molten polystyrene samples show negligible expansion when going from 120 to 240 °C.[49] As a final point for this discussion, Tangari *et al.*[24] mention that no change in scattering was observed for a bimodal blend at 120 and 35 °C. It is concluded that differences due to temperature effects can be dismissed.

B. Analysis of Chain Swelling−Radius of Gyration. As stated in the introduction, a simple criterion divides the molecular weight pairs into two regimes: swollen and unswollen. The scaling hypothesis in eq 7 is written in terms of a hypothetical step length b. It becomes a question when analyzing experimental data what value for b should be used to determine the crossover molecular weight. The approach here is to use the Kuhn segment molecular weights M_K for calculating the number of segments P and N. On the basis of the characteristic ratio $C_\infty \cong 10$ for polystyrene,[49,50] M_K is 520 for hPS and 560 for dPS.[51] Therefore, the number of *Kuhn segments* for the host and guest polymers are listed in Table 1 under the columns headings P and N, respectively. The approximate matrix crossover point for each of the dPS samples can be calculated from eq 7. Even with this definition, there are several blends in which the distinction of swollen/unswollen is questionable, as evidence of swelling is often detected at somewhat higher host molecular weights. However, the conclusions reached from the results that follow are not affected by this concern.

It is apparent from the data in Table 2 that the longer guest chain does indeed swell when the host's molecular weight is decreased. Figure 4 tests the molecular weight dependence of R_g according to eq 8 for blend pairs that are nominally in the swollen regime. Here, the dimension of the longer guest chain, adjusted by $P^{1/5}$ to renormalize the excluded volume effect of the shorter chain, is plotted as a function of the number of dPS segments N on a double-log scale. Included in the figure are two data points from the study of Tangari *et al.*[24] The most fully swollen long chain of the blend pairs from Table 2 are used in a linear least-squares fit to produce the solid line, which has a slope of 0.61 ± 0.03. Although the renormalization factor $P^{1/5}$ does not collapse all of the R_g values to a common point for each long chain, the slope is in accord with the scaling exponent of 3/5. The same data are replotted in Figure

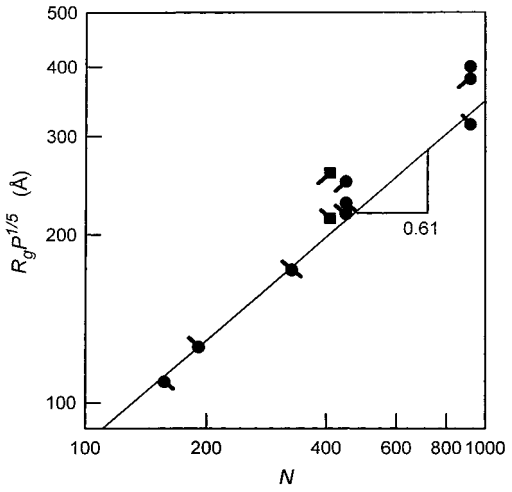

Figure 4. Double-logarithmic plot of the long chain R_g, adjusted by $P^{1/5}$ to renormalize for the excluded volume effect of the shorter chain, versus the number of segments N. Included in the figure are two data points (squares) from the study of Tangari *et al.*[24] Only the blend pairs that fall into the *swollen* category are shown. The different pip symbols delineate the various short chain solvents P for each long chain solute N (see the upper half of Table 1).

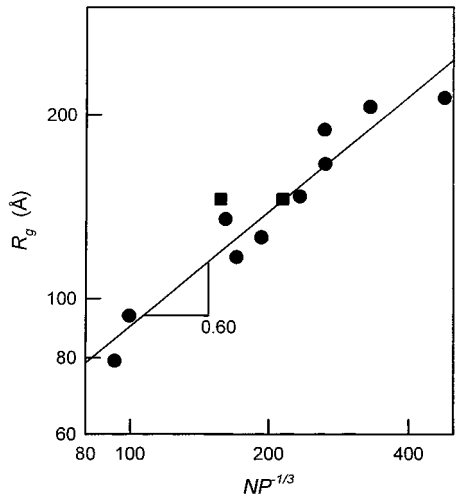

Figure 5. Same data from Figure 4 replotted as log R_g vs log $NP^{1/3}$ to change the scaling emphasis from the ordinate to the abscissa. A linear least-squares fit to *all* points produces an exponent of 0.60 ± 0.07, represented by the solid line.

5, as log R_g vs log $NP^{1/3}$ to change the rescaling emphasis from the ordinate to the abscissa; a linear least-squares fit to *all* points produces an exponent of 0.60 ± 0.07.

The assumption, of course, in the above analysis is that the renormalization of the long chain R_g by the factor $P^{1/5}$ to account for screening by the short polymer solvent of excluded volume, as stated in eq 8, is valid. To test this assumption, the data from the swollen regime have been plotted as $R_gN^{-3/5}$ vs P in Figure 6 on a double-log scale. The linear least-squares fit to the data from this study produces a weaker dependence on P, with a power law exponent of −0.098 ± 0.020. If one now employs this recalculated value to correct for a weaker excluded volume screening effect as in Figure 7 as log $R_gP^{0.098}$ vs log N, the originally determined exponent is changed slightly to 0.588 ± 0.024 (or 0.586 ± 0.030 if the data from ref 24 are included). One effect that this adjustment in the renormalization has is that most of the long chain radius of gyration data nearly collapses to a single point for a given long chain

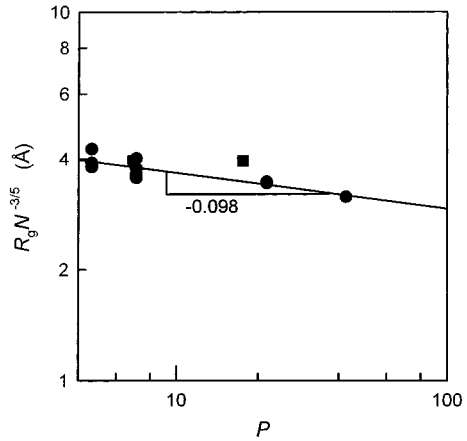

Figure 6. Data from the swollen regime plotted as $R_gN^{-3/5}$ vs P on a double-log scale to check for the weak screening of the host short polymer. The linear least-squares fit produces a weaker dependence than $P^{-1/5}$, with a power law exponent of −0.098 ± 0.020.

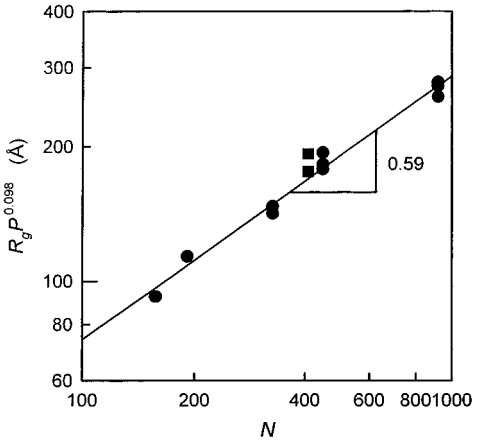

Figure 7. Reanalysis of the data from Figure 4 using the recalculated exponent for P from Figure 5, with log $R_gP^{0.098}$ plotted against log N. Note that the data nearly collapse to a single point with the weaker revised screening adjustment. Because of the significant overlap of data, the pips from Figure 4 have been removed.

molecular weight (compare Figure 4 against Figure 7). Even more remarkable is that the guest chain's excluded volume exponent of 0.588 is exactly the same as the one determined from precise perturbation calculations.[2] The significance of finding a weaker screening exponent for the short chain P, that is $-1/10$ instead of $-1/5$, is indicated further on.

The R_g data from the blends in the unswollen regime are displayed in Figure 8 in a log−log plot according to eq 9, along with one point from Tangari *et al.*[24] It is evident that the data approaches the power law exponent of $1/2$, as required for unperturbed chains, with the least-squares slope of 0.504 ± 0.009. The data are in close agreement with the dashed line, which represents the empirical fit for polystyrene,[26] $R_g(\text{SANS}) = 0.267M_w^{1/2}$. When fit according to the same format, the equation for the solid line in Figure 8 is

$$R_g = 0.252M_{w,dPS}^{0.504} \quad (17)$$

Second Virial Coefficient. Although the scaling of A_2 for host molecular weight has been theoretically postulated[21] in eqs 8 and 9, this work represents the first systematic experimental study of its scaling behavior in bimodal blends. For the case of an unswollen

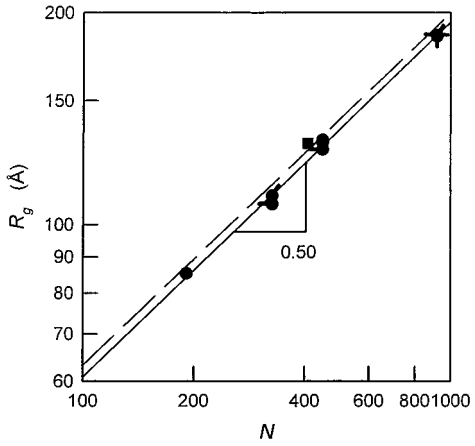

Figure 8. R_g data from the blends in the *unswollen* regime displayed in a log−log plot according to eq 9, along with one point (square) from Tangari *et al.*[24] The dashed line represents the empirical fit for polystyrene from the literature (see text). The symbols are listed in the upper half of Table 1.

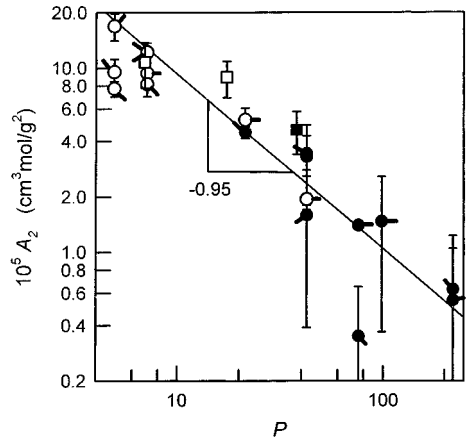

Figure 9. Second virial coefficient A_2 plotted against the short chain length P for *all* of the data from Table 2. The filled points are for the blends fulfilling the unswollen criterion, as according to eq 9, and the solid line has a slope of 0.95 ± 0.24. The symbols designate the different long guest chains and are summarized in the lower half of Table 1. The squares are from the study of Tangari *et al.*[24]

guest chain, scaling arguments suggest that A_2 is proportional to the reciprocal host chain length according to eq 9; *all* of the data from Table 2 are plotted in Figure 9.[52] The filled points are for the blends fulfilling the unswollen criterion, and the solid line has a slope of 0.95 ± 0.24, which represents the unweighted linear least-squares fit to the same data; when weighted for uncertainty, the fit produces a scaling exponent of 0.91 ± 0.25, which is not shown in the figure. Despite the large relative uncertainties in A_2, on account of being determined by only three concentrations and also due to their small values, the scaling result is satisfactory.

Figures 10 and 11 represent all of the second virial coefficient data according to eq 8, where the open symbols are for the swollen long chains. In Figure 10, A_2 has been multiplied by $N^{1/5}$ to rescale for excluded volume. A −0.58 ± 0.12 power law, close to $-3/5$, is shown by the solid line in the figure. The data represented in Figure 11 have a different emphasis (analogous to Figure 4; cf. Figure 5), A_2 vs $PN^{1/3}$, so as to eliminate the overlap of the independent variables. A linear least-squares fit to the open symbols results in a slope of −0.59 ± 0.10. It is noted here that an attempt to experimentally determine the scaling exponent for N used to rescale the second virial coefficients (*i.e.*, from

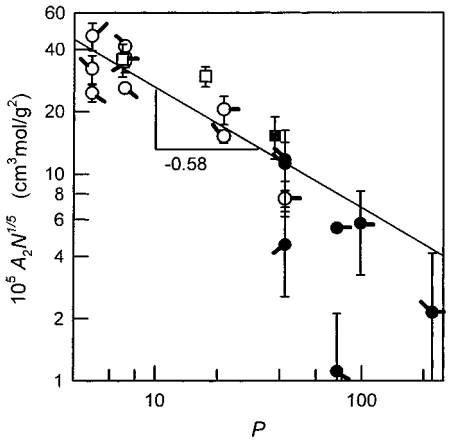

Figure 10. Plot of $A_2N^{1/5}$ vs P (short chain length) where the rescaling of A_2 accounts for the excluded volume effect. The open circles are for the swollen long chains, and the −0.58 power law slope is drawn through the data according to eq 8. The symbols are the same as in Figure 9.

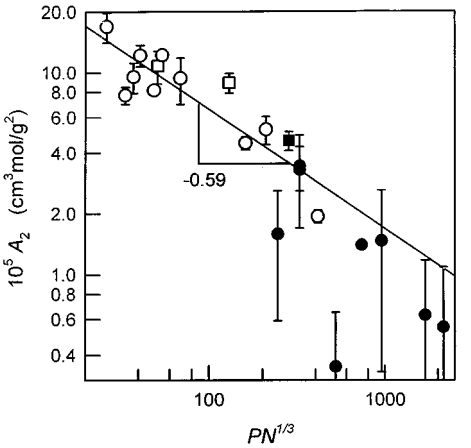

Figure 11. Same data as in Figure 10 with a different scaling emphasis, A_2 vs $PN^{1/3}$. A linear least-squares fit to the open symbols results in a slope of −0.59 ± 0.10.

a plot of $A_2P^{3/5}$ vs N as in the swollen R_g data of Figure 6) resulted in a plot with substantial scatter having a measured power law slope of −0.21 ± 0.15 (plot not shown). Given the large relative uncertainty of the determination, it is deemed fortuitous that the value is nearly identical to the assumed exponent of $-1/5$ (eq 8); hence, for the lack of a more precise value only the evaluation for the P exponent is made.

Admittedly the scatter in the virial coefficient data of Figures 9−11 is such that one could argue a single power law fit may be sufficient over the entire range of short chain molecular weights. However, the test is to determine whether the scaling concepts that are acceptable for the radius of gyration are viable. The tendency is for the data in the unswollen region (filled circles, Figures 10 and 11) to fall below the trend of the swollen blends and for the open points in Figure 9 representing the swollen guest polymer regime to fall below the predicted line for the unswollen regime.

Crossover of $S(q)$. According to eqs 2 and 5, the structure factor $S(q)$ scales as q^{-2} for unswollen guest chains and as $q^{-5/3}$ for swollen ones, respectively. The unswollen dependence has been observed in conventional small molecule solvents at the Θ-temperature and in a melt of similarly sized dPS/hPS chains, as mentioned in the introductory section. Figure 12 presents the SANS profiles for two of the blends containing the longest guest chain, D2950, dissolved in the H2000 and

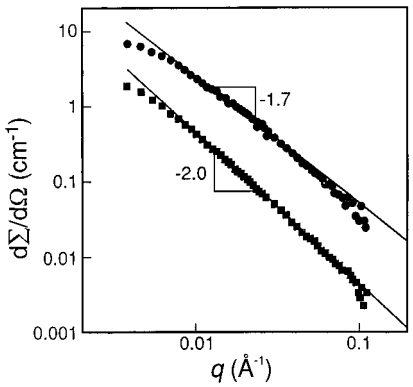

Figure 12. Double-logarithmic plot of the SANS profiles for two of the blends containing the longest guest chain, D2950, dissolved in the H2000 (squares, lower curve) and H3.69 (circles, upper curve) hosts. The segment−segment correlations of the guest chain in the D2950/H2000 mixture are unperturbed as seen by the −2 power law, whereas excluded volume interactions prevail for the blend with the shortest host as seen from the −1.7 scaling exponent.

H3.69 hosts. The data were measured with two sample-to-detector distances in the 30 m SANS instrument to provide a large scattering vector range and have been shifted vertically from one another for easier viewing. It is quite reasonable to conclude that the segment−segment correlations of the guest chain in the D2950/H2000 mixture are unperturbed (−2.0 power law), whereas excluded volume interactions prevail for the blend with the shortest host as seen from the −1.7 scaling exponent. The deviation at low q is a result of the single chain structure and perhaps intermolecular correlations even at the very low, but finite, concentration of 0.5 wt %.

The transition from random walk to excluded volume statistics and the observation of a molecular weight dependent crossover between the unswollen and the swollen regimes can be seen with the data displayed in a Kratky plot, $q^2(d\Sigma/d\Omega)$ vs q. Figure 13 is for the bimodal blend series with the long chain D2950 at 0.5 wt %, and Figure 14 is for D514 at 2.0 wt %. The counting statistics for the D514 blends is considerably better because of the difference in the perdeuterated chain concentration. The sequence of the scattering curves is such that the molecular weight of the shorter chain is successively decreased as one proceeds from top to bottom; the short chain molecular weights are given in the figure captions. The uppermost and bottommost scattering curves in Figures 13 and 14 are combined from two sample-to-detector distances, 15 and 3 m. Finally, each of the solid lines is calculated for the ideal Gaussian chain having an R_g of 442 Å (Figure 13) and 186 Å (Figure 14) using the empirical relationship from eq 17 and the Debye equation (eq 11).

The topmost profiles in each figure indicate that the guest chain is nominally ideal in the D2950/H2000 and D514/H180 blends. As the host molecular weight is decreased, the correlation amongst monomers of the long guest chain deviates from that of a random walk and the crossover point in reciprocal space moves with the short chain size. The apparent molecular weight dependence of this crossover will be discussed more in-depth shortly.

The exercise of replotting the data in a modified Kratky form of $q^{5/3}(d\Sigma/d\Omega)$ vs q to determine whether there is an intermediate plateau proved not as revealing due to a departure on the low q side from the single chain shape factor as well as from the change in the

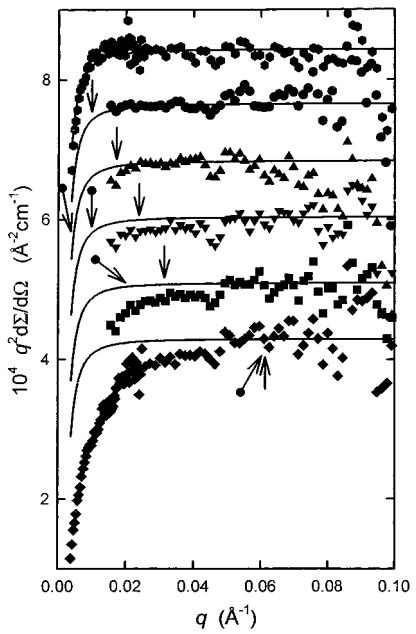

Figure 13. Kratky plot for the bimodal blend series with the long chain D2950 at 0.5 wt %. From top to bottom, the short chain molecular weights are H2000, H115, H39.4, H22.1, H11.2, and H3.69. The solid curves are calculated for an unperturbed coil having an R_g of 448 Å, and, as with the experimental data, have been shifted vertically for clarity. The solid arrows designate the expected crossover point where $qR_g(\text{short}) = 1$; the arrows with the dot tip are for $q\xi(\text{short}) = 1$ (see text for discussion).

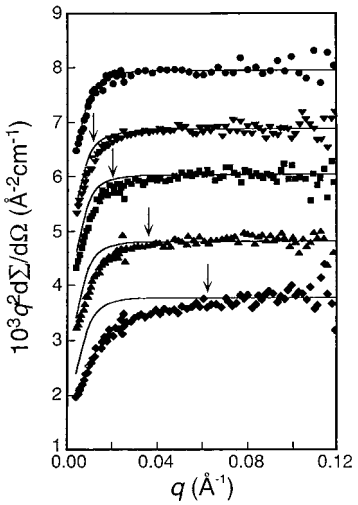

Figure 14. Kratky plot for the bimodal blend series with the long chain D514 at 2 wt %. From top to bottom, the short chain molecular weights are H180, H115, H39.4, H11.2, and H3.69. The solid curves are for an ideal chain with $R_g = 186$ Å, and the crossover points mark where $qR_g(\text{short}) = 1$.

segment−segment correlation. It is difficult to precisely determine whether the scaling exponent of −1.7 (*i.e.*, $-5/3$) found in Figure 12 holds for the remaining blends. Nevertheless, it is distinctly clear that the crossover from ideal to swollen chain behavior depends on the short chain molecular weight. We note that the crossover analysis is restricted to $q \leq 0.1$ Å^{-1} in keeping with the cautionary note that chain rigidity effects become important for polystyrene.[14]

IV. Discussion and Summary

***q*-Dependent Crossover in *S*(*q*).** The expansion of a single long polymer chain in a sea of shorter, chemically identical chains was first proposed by Flory over

40 years ago. Recent theoretical treatments have been advanced to address the phenomenon with scaling arguments. Although past studies have qualitatively confirmed the observation of chain swelling, experimental support for any of the scaling predictions cited in eqs 8 and 9 has been lacking. The transition from ideal to excluded volume statistics rests with the concept of a short chain-dependent screening length, or blob size ξ. For distances smaller than ξ, the short chains screen the excluded volume interactions between the long chain's segments, leading to an ideal conformation. At larger length scales the long chain is made up of these screened blobs with excluded volume interaction between them.[20]

The main assumption in determining the crossover transition is given in eq 7; that is, the long chain only starts swelling when its number of segments N exceeds the *square* of the number of segments in the short chain. Taken another way, the screening blob size depends on P as

$$\xi \sim P \tag{18}$$

For the sake of this discussion, which will become clearer shortly, let us also consider the possibility that the screening length tracks as the radius of the short chain, *i.e.*, as $P^{1/2}$. Unfortunately, without the proportionality constant relating ξ to P (or ξ to $P^{1/2}$), it is difficult to pinpoint the crossover in q-space ($\sim 1/\xi$) to make the comparison.

If one assumes that the screening length is equal to the short chain radius of gyration, then it is a straightforward matter to calculate where the crossover in $S(q)$ occurs. In fact, the solid arrows (without dotted ends) in Figures 13 and 14 have been calculated for $qR_g(P) = 1$, where $qR_g(P)$ is for the shorter matrix chains, calculated from eq 17 for polystyrene; thus, the solid arrows are for the screening length $\xi \sim P^{1/2}$. To make the like evaluation for the $\xi \sim P$ assumption, the screening length is set equal to $R_g(P = 7)$ and the bottom curves of Figure 13 and a proportionality constant for eq 18 are estimated. For the remaining curves, the arrows with the dotted end indicate where the crossover should be for each (*i.e.*, $q\xi(P) = 1$) of the short chain molecular weights using this proportionality constant. Note how these marks rapidly move to lower q with increasing short chain length, because the screening effect occurs at significantly larger length scales than the short chain radius. The precise position of the crossover when $\xi \sim P$ is contingent, of course, on the arbitrary assignment stated above. However, the crossover transition in reciprocal space appears to vary more realistically with $\xi \sim P^{1/2}$ rather than $\xi \sim P$.

Scaling Exponent. Summing up to this point, the crossover trends seem to better follow

$$\xi \sim P^{1/2} \quad (i.e., \xi \sim R_g) \tag{19}$$

which has the following effect on the scaling relationship for the long chain. The long chain is considered to be a string of blobs of step length ξ and having g ($= P$) monomers, with $\xi \sim g^{1/2} \sim P^{1/2}$. The swollen long chain radius will now scale as[20]

$$R \sim (N/g)^{3/5}\xi \tag{20}$$

meaning that

$$R \sim N^{3/5}P^{-1/10} \tag{21}$$

in contrast to the prediction of eq 8 where ξ goes as P, or

$$R \sim N^{3/5}P^{-1/5} \tag{22}$$

Interestingly, the smaller exponent for P more properly accounts for the data shown in Figures 6 and 7, when contrasted with the representation in Figure 4.

For the first time this work confirms several of the scaling predictions for a guest chain's radius of gyration and second virial coefficient as functions of its own length and the length of the lower molecular weight polymeric solvent. Moreover, a crossover in the segment−segment correlation function shows that the long chain behaves as an ideal random walk chain at short distances and has an excluded volume trajectory for longer distance scales. A new finding, however, is that the position of the crossover appears to depend on R_g of the shorter chain, or $P^{1/2}$ rather than P.

Thus, for a swollen long chain of length N in a melt of short chains P, one observes

$$R_g \sim N^{0.588\pm0.024}P^{-0.098\pm0.020} \tag{23}$$

$$A_2 \sim N^{-1/5}P^{-0.59\pm0.10} \tag{24}$$

The relationship $S(q) \sim q^{-5/3}$ for the long chain is maintained for the spatial crossover point $qR_g(P) < 1$, which is consistent with the revised molecular weight scaling for P in eq 23. The characteristic ideal chain behavior is recovered at a new crossover point, that is when $P > N$, with

$$R_g \sim N^{0.504\pm0.009} \tag{25}$$

$$A_2 \sim P^{-0.95\pm0.24} \tag{26}$$

and $S(q) \sim q^{-2}$ for $qR_g(\text{short}) > 1$.

One final comment concerning the study is that the hPS crossover point noted in Table 1 is slightly affected by the revised molecular weight crossover. There are only one or two blends from the table that were originally considered "unswollen" to now be taken into account as being "swollen". Hence, the effect on the calculated scaling exponents from eqs 23−26 is minimal.

Acknowledgment. The author would like to thank M. Rubinstein, J. O'Reilly, and especially R. Colby for many fruitful discussions related to scaling concepts and SANS data analysis. The help of C. Glinka, C. Han, J. Barker, and B. Hammouda of the NIST SANS facility is gratefully recognized.

References and Notes

(1) Flory, P. J. *J. Chem. Phys.* **1949,** *17*, 303.
(2) des Cloiseaux, J.; Jannink, G. *Polymers in Solution*; Clarendon Press: Oxford, England, 1990.
(3) For example, see: de Gennes, P. G. *Scaling Concepts in Polymer Physics*; Cornell University Press: Ithaca, NY, 1979.
(4) Flory, P. J. *Principles of Polymer Chemistry*; Cornell University Press: Ithaca, NY, 1953.
(5) Fukuda, M.; Fukutomi, M.; Kato, Y.; Hashimoto, T. *J. Polym. Sci., Polym. Phys.* **1974**, *12*, 871.
(6) Miyaki, Y.; Einaga, Y.; Fujita, H. *Macromolecules* **1978,** *11*, 1180.
(7) Cotton, J. P.; Decker, D.; Benoit, H.; Farnoux, B.; Higgins, J. S.; Jannink, G.; Ober, R.; Picot, C.; des Cloiseaux, J. *Macromolecules* **1974,** *7*, 863.
(8) Kirste, R. G.; Kruse, W. A.; Ibel, K. *Polymer* **1975,** *16*, 120.
(9) Wignall, G. D.; Ballard, D. G. H.; Schelten, J. *Eur. Polym. J.* **1974,** *10*, 861.

(10) Durchschlag, H.; Kratky, O.; Breitenbach, J. W.; Wolf, B. A. *Monatsh. Chem.* **1970,** *101*, 1462.
(11) Edwards, S. F. *Proc. Phys. Soc.* **1965,** *85*, 613.
(12) Rigorous renormalization group theories, as for example cited in reference 2, have established the exponent in eq 6 to be $\nu = 0.588$, and conversely, in eq 5 to be $-1/\nu = -1.701$. For the results presented in this paper, the approximate scaling exponents will suffice.
(13) Cotton, J. P.; Decker, D.; Farnoux, B.; Jannink, G.; Ober, R.; Picot, C. *Phys. Rev. Lett.* **1974,** *32*, 1170.
(14) Rawiso, M; Duplessix, R.; Picot, C. *Macromolecules* **1987,** *20*, 630.
(15) Cotton, J. P. *J. Phys. Lett.* **1980,** *41*, L-231.
(16) Daoud, M; Jannink, G. *J. Phys.* **1976,** *37*, 973.
(17) Farnoux, B.; Boué, F.; Cotton, J. P.; Daoud, M.; Jannink, G.; Nierlich, M.; de Gennes, P. G. *J. Phys.* **1978,** *39*, 77.
(18) de Gennes *J. Polym. Sci., Polym. Symp.* **1977,** *61*, 313.
(19) (a) Joanny, J. F; Grant, P.; Pincus, P.; Turkevich, L. A. *J. Appl. Phys.* **1981,** *52*, 5943. (b) Joanny, J. F.; Grant, P.; Turkevich, L. A.; Pincus, P. *J. Phys.* **1981,** *42*, 67.
(20) Daoud, M; Family F. *J. Phys.* **1984,** *45*, 151.
(21) Nose, T. *J. Phys.* **1986,** *47*, 517.
(22) Raphael, E.; Fredrickson, G. H.; Pincus, P. *J. Phys. II Fr.* **1992,** *2*, 1811.
(23) Kirste, R. G.; Lehnen, B. R. *Makromol. Chem.* **1976,** *177*, 1137.
(24) Tangari, C.; Ullman, R.; King, J. S.; Wignall, G. D. *Macromolecules* **1990,** *23*, 5266.
(25) O'Connor, K. M.; Pochan, J. M.; Thiyagarajan, P. *Polymer* **1991,** *32*, 195.
(26) Tangari, C.; King, J. S.; Summerfield, G. C. *Macromolecules* **1982,** *15*, 132.
(27) Kent, M. S.; Tirrell, M.; Lodge, T. P. *Macromolecules* **1992,** *25*, 5383.
(28) Brochard, F.; de Gennes, P.-G. *Europhys. Lett.* **1986,** *1*, 221.
(29) de Gennes, P.-G. *Macromolecules* **1986,** *19*, 1245.
(30) Colby, R. H. Submitted to *J. Phys. II (Fr.).*
(31) Green, P. F.; Kramer, E. J. *Macromolecules* **1986,** *19*, 1108.
(32) Seggern, J. v.; Klotz, S.; Cantow, H.-J. *Macromolecules* **1989,** *22*, 3328.
(33) Glinka, C. *J. AIP Conf. Proc.* **1981,** *No. 89*, 395.
(34) $d\Sigma(0)/d\Omega$ for the silica calibration standard was originally reported as 28.4 cm^{-1} in 1986 for the 8 m SANS instrument. However, its value was revised to 32.0 cm^{-1} for the later studies, and so the earlier data were corrected for the change.
(35) Zimm, B. H. *J. Phys. Chem.* **1948,** *16*, 1093.
(36) Ullman, R. *J. Polym. Sci.: Polym. Lett. Ed.* **1983,** *21*, 521.
(37) Ullman, R. *J. Polym. Sci.: Polym. Phys. Ed.* **1985,** *23*, 1477.
(38) Debye, P. *J. Phys. Colloid Chem.* **1947,** *51*, 18.
(39) Lodge, T. P.; Hermann, K. C.; Landry, M. R. *Macromolecules* **1986,** *19*, 1996.
(40) Matsushita, Y.; Noda, I.; Nagasawa, M.; Lodge, T. P.; Han, C. C.; Amis, E. J. *Macromolecules* **1984,** *17*, 1785.
(41) King, J. S.; Boyer, W.; Wignall, G. D.; Ullman, R. *Macromolecules* **1985,** *18*, 709.
(42) Witten, T. A.; Schaefer, L. *J. Chem. Phys.* **1981,** *74*, 2582.
(43) Ohta, T.; Oono, Y.; Freed, K. F. *Phys. Rev.* **1982,** *25*, 2801.
(44) Briber, R. M.; Bauer, B. J.; Hammouda, B. *J. Chem. Phys.* **1994**, *101*, 2592.
(45) Buckingham, A. D.; Hentschel, H. G. E. *J. Polym. Sci., Polym. Phys. Ed.* **1980,** *18*, 853.
(46) Bates, F. S.; Wignall, G. D. *Macromolecules* **1986,** *19*, 932.
(47) Bates, F. S.; Wignall, G. D. *Phys. Rev. Lett.* **1986,** *57*, 1429.
(48) Richardson, M. J.; Savill, N. G. *Polymer* **1977,** *18*, 3.
(49) Boothroyd, A. T.; Rennie, A. R.; Wignall, G. D. *J. Chem. Phys.* **1993,** *99*, 9135.
(50) Flory, P. J. *Statistical Mechanics of Chain Molecules*; Hanser Publishers: New York, 1969.
(51) C_∞ is equivalent to the number of backbone bonds in the Kuhnian segment. Therefore, the number of monomers in the same segment is $C_\infty/2$ for polystyrene.
(52) The second virial coefficient data of Tangari *et al.* from ref 24 are included; however, it appears that their values differ by a factor of 2 from the ones in this study so their results have been adjusted accordingly.

MA970270A